Annual Progress Report

NASA Grant NAG5-32 MASTER

1 June 1987 - 31 May 1988

between NASA

and

The Department of Earth and Planetary Sciences
The Johns Hopkins University, Baltimore, Maryland 21218

entitled

"The Delineation and Interpretation of the Earth's Gravity Field"

Principal Investigator:
Bruce D. Marsh
Dept. of Earth and Planetary Sciences
The Johns Hopkins University
Baltimore, Maryland 21218

Abstract

A series of fluid dynamical experiments in variable viscosity fluid have been made and are in progress to study: (1) the onset of small scale convection relative to lithosphere growth rate; (2) the influence of paired fracture zones in modulating the horizontal scale of small scale convection; (3) the influence of the mantle vertical viscosity structure on determining the mode of small scale convection; and (4) the three dimensional and temporal evolution of flows beneath a high viscosity lid. These experiments extend and amplify our present experimental work that has produced small scale convection beneath a downward-moving solidification front. Rapid growth of a high viscosity lid stifles the early onset of convection such that convection only begins once the lithosphere is older than a certain minimum age. The interplay of this convection with both the structure of the lithosphere and mantle provide a fertile field of investigation into the origin of geoid, gravity, and topographic anomalies in the central Pacific. These highly correlated fields of intermediate wavelength (~ 200-2000 km) show isostatic compensation by a thin lithosphere for shorter ($\leq$ ~ 500 km), but not the larger, wavelengths. It is the ultimate, dynamic origin of this class of anomalies that is sought in this investigation.

1. Introduction

Intermediate to short wavelength (i.e. ~ 200-2000 km) geoid and gravity anomalies over the ocean basins result from the structure and mechanical behavior of a growing lithosphere and its interaction with thermal convection within the underlying mantle. Because of the existence of a low seismic velocity zone immediately beneath much of the earth's lithosphere - due to the grazing of the mantle solidus by the geotherm - a geometrically similar low viscosity region may also exist that preferentially promotes flow. The flow itself is driven in the earliest stages by strong cooling from the top, with concomitant growth of the lithosphere, and much later by heating from the deeper mantle. The characteristic vertical length scale of this small scale flow is set by the viscosity structure within the uppermost mantle. Much attention is now being paid to how soon this small scale flow develops with distance from the ridge (Buck and Parmentier, 1986), to the evolution of the vertical structure (Robinson and Parsons, 1988), and to the thermal role of fracture zones in modulating the flow (Craig and McKenzie, 1986; Driscoll and Parsons, 1988). All of this work has been numerical whereas ours centers around a set of actual laboratory experiments to compliment and extend these earlier results.

Of the abundance of earlier work on variable viscosity convection beneath a growing, highly viscous rigid lid (e.g. Parsons and McKenzie, 1978; Yuen et al., 1981; Yuen and Fleitout, 1986; Fleitout and Yuen, 1984; Jaupart and Parsons, 1985; among others above), a common element has been either the demonstration or

utilization of the fact that the flow is generally confined to a region across which the viscosity changes by no more than a factor of about 10. The associated lithosphere for such a flow, therefore, is that part of uppermost fluid whose viscosity is greater than ten times that of the underlying fluid. The fact that the low viscosity zone (LVZ) extends downward perhaps no more than 200-300 km further limits the vertical structure, although Robinson and Parsons (1988) suggest that this zone itself may as a unit become unstable and yield yet another, larger class of instabilities that stir the mantle to perhaps 600 km. The horizontal length scale would normally also be set by this vertical structure were it not for the thermal irregularities in the lithosphere itself.

Age differences across fracture zones mean differences in plate thickness, which also cause differences in vertical heat flow. These differences give rise to horizontal temperature gradients that force a horizontal flow normal to fracture zones. This imposed upper thermal structure may strongly influence the flow, with cells forming on each side of the fracture zone. Craig and McKenzie (1986) have modeled this effect for a single fracture zone. The third feature that sets the scale of the flow is the thickness of the unstable thermal boundary layer at the leading edge of the growing lithosphere, from which the initial plumes grow. This has been investigated by Buck and Parmentier (1986) in an approximate, but revealing, fashion; the scale and vigor of the flow change with time.

It is the role of these three features, namely, vertical viscosity structure, fracture zones, and growth rate of the lithosphere, in controlling small scale mantle convection that we continue

experimentally to investigate. In addition, the unsteady and 3-dimensional nature of the flow is being investigated.

We next proceed to summarize our work on this general subject over the past year or so and in the following section 3 give a more detailed statement of the future direction of this work.

2. Present and Past Work

Over the past year we have conducted a series (43) of fluid dynamical experiments to study the onset of convection in variable viscosity fluid undergoing cooling from above. Growth of the lithosphere has been simulated by using molten paraffin and cooling it from above to below its melting point. Two types of paraffin involving nearly pure n-nonadecane (m.p. = 32°C) and a similar mixture has allowed simulation of a solidus-liquidus relationship, with a significant mush zone of 4-5°C, much like expected for the mantle. The experimental set up is shown schematically by Figure 1: Two plexiglass tanks with thick walls (2 cm) 20 x 20 x 20 cm and 20 x 20 x 10 cm capped by a copper and aluminum cooling jacket have been employed. The Rayleigh number for these experiments, based on the tank thickness, can be varied between about 10^5 and 10^9, depending on the exact fluid used and tank thickness, which thus covers the expected value of Ra for the earth. Although it is still premature to give a full report, some typical results are shown by Figure 2. (Aluminum flakes and time-lapse photographs give a sense of the motion).

The run begins with an isothermal tank of fluid, which has been heated from below to attain this state. The tank is inverted and its upper boundary temperature is suddenly dropped and held below the fluid melting point. A frost or thin crust immediately forms. Several minutes later a series of small plumes, spaced at 1 - 2 cm, descend from the roof and travel downward 2-3 cm before dissipating. A second series of larger plumes form next, travel further downward and cause a general, deepseated stirring. After 5-10 minutes a general cellular form of convection is established that extends downward in direct proportion to the amount of superheat in the system. With small superheat (~ 1°C), the flow always resides in the upper part of the tank, against the downward growing crust, while the lowermost fluid remains motionless. These are the first experiments, to our knowledge, that clearly show the feature of small-scale convection during growth of a rigid (i.e. lithospheric-like) lid.

The overall vigor of the flow is directly proportional to the amount of superheat in the system, and as soon as this superheat is lost (Fig. 2, upper) convection ceases. The crust continues to grow into a now stagnant layer of fluid that shows no signs of crystallization whatsoever. Both the loss of superheat and the thickening of the crust (causing retardation of cooling) contribute to slow convection. Overall these results are broadly similar to that found numerically by Buck and Parmentier (1986). More on these experiments and proposed extensions will be given in the following section, but first we give a brief overview of our research program.

Over that past ten years our plan has been first to delineate the gravity and geoid fields in the Pacific, with particular emphasis on anomalies of intermediate wavelength (n,m $\approx$ 18-22, $\lambda \approx$ 2000 km), and then to interpret these anomalies in relation to the dynamics of the lithosphere and upper mantle (e.g. Marsh and Marsh, 1976). The method of satellite to satellite tracking (SST) was used to delineate these anomalies over the central Pacific (e.g. Marsh et al., 1981). And with the complementary data from SEASAT (e.g. Marsh et al., 1984) this anomaly set has become well established. But because some workers (e.g. Sandwell, pers. com.) have felt that these anomalies could, at least in part, be artifacts of truncating spherical harmonic expansions to remove the long wavelength (i.e. regional) effects, we have also continued research along these lines (see more below). Having established this class of anomalies, we have worked at understanding or interpreting them in terms of the isostasy of the lithosphere and convection within the underlying mantle. (Marsh and Hinojosa, 1983; Marsh et al., 1984; Hinojosa and Marsh, 1985; Hinojosa, 1986.)

We have found that the most direct way to show the unequivocal existence of these anomalies is to take the full geoid (untruncated) of the central pacific and remove a simple (first, second, or third order) surface. It is important to realize that the removed surface is not a spherical harmonic field but merely a cartesian surface, which is possible over this limited area. The resultant residual geoid is exceedingly similar to that found by removing a spherical harmonic field model (n, m $\leq$ 12,12), see Figures 3 and 4. The same has been done for the bathymetry in this region,

and the geoid and bathymetry have been plotted against one another (Figure 5), which gives a clear positive correlation (corre.. coef. = 0.66) The slope of this correlation is also highly significant (i.e. ≈ 7.5 m/km) in that it is very close to the spectrally derived admittance (see below). Altogether we are confident that this class of anomalies is real. Another class of anomalies, of shorter wavelength (~ 200 km), has been singled out by Haxby and Weissel (1986) in the southern Pacific as being indicative of mantle convection, but there is concern about their origin (more later).

By treating both bathymetry and geoid in the spectral or wave number domain, the admittance has been obtained from the ratio of the geoid to the topography, which expresses the geoid anomaly in meters for every kilometer of sea-floor topography (Figure 6). The phase has also been found and it is always positive and generally small. Synthetic admittance both for flexural and Airy compensation models have also been calculated and are shown along with the observed admittance of Figure 6. It is clear here that wavelengths shorter than about 1000 km can be compensated both regionally, by the elastic strength of the lithosphere itself, and locally by displacing mantle material to reach isostatic equilibrium. The larger wavelengths, however, cannot be explained in this fashion but must be supported dynamically within the sublithospheric mantle.

To investigate this dynamic process of compensation, Hinojosa (1986) has numerically studied the effect of convection of a variable viscosity fluid, cooled from above and heated from below on deformation of the lithosphere. Using the mean field method, with and without inclusion of a low viscosity channel, the geoid,

topography, and admittance have been calculated as a function of time (see Figure 7). Although the results of this study are far too numerous to be included here, the central result is that small scale convection by itself is not strong enough to produce significant geoid and topographic anomalies that also satisfy the observed admittance. (Buck and Parmentier (1986) show that the geoid can be matched but they did not notice the problem with admittance.) But that regional thermal variations, originating, for example, at the ridge itself, carried along by the flow can cause anomalies of the observed magnitude (see Appendix A). For example, Figure 8 shows contours of geoid anomaly magnitude as a function of thermal anomaly depth and amplitude. The same has been done for topography and both results have been combined through admittance to reveal the acceptable range of thermal anomaly amplitude and depth. The critical range is 70-100°C at depths of, respectively, 100-200 km.

All of this work is now being readied for publication.

3. Present and Future Direction of Research

That small scale convection is likely to exist beneath the Pacific plate is hardly anymore doubted. But its form and how it relates to the structure and dynamics of the lithosphere remains enigmatic. In this regard we are investigating three topics:

(1.) The relation of the onset time of convection to the rate of lithosphere growth. How close to the ridge does convection begin and when does it cease.

(2.) What is the influence of paired fracture zones on modulating or styling the convection to the structure of the lithosphere.

(3.) How does the vertical viscosity stratification confine and regulate the flow.

(4.) What is the three dimensional structure and long-term evolution of the flow field.

All of these topics revolve around the means by which the scale of small scale convection is set by the lithosphere and viscous regime of the uppermost mantle. Understanding this scale of motion provides insight into understanding the origin of the geoid and gravity anomalies in oceanic regions.

As mentioned in the Introduction a recent number of works (e.g. Buck and Parmentier, 1986; Craig and McKenzie, 1986; Robinson and Parsons, 1988) have considered this general topic from a numerical point of view. They have been motivated to explain the short wavelength class of geoid anomalies in the south central pacific singled out by Haxby and Weissel (1986). These anomalies are oriented roughly parallel to the direction of absolute motion and have a characteristic wavelength of about 200 km; they have a gravity signature of about 10 mGals. A recent detailed study of the spectral characteristics of these anomalies and the associated lithosphere by McAdoo and Sandwell (1988) suggests that they are not dynamically supported. They are, however, consistent with models of flexural isostatic compensation by a very thin lithosphere. If so, the only obvious class of anomalies left requiring systematic explanation is that with wavelengths near ~ 2000 km and roughly

bounded by the major fracture zones (Marsh, et al., 1984) which are distinct from those associated with swells or hot spots. It is this spatial scale that we find of particular interest.

The main difficulty in numerical experiments is that the viscosity structure is not accurately modeled. Generally, two or more isoviscous layers are assumed covered by a rigid, conducting lid of given (and invariant) thickness (e.g. Robinson and Parson, 1988; Craig and McKenzie, 1986). In light of the work by Booker and Stengel (1976) and Richter et al. (1983), it is clear that in systems with strong variations in viscosity the flow is confined to a region where the viscosity varies by less than a factor of 10; the flow is across an essentially isoviscous region. This allows the system to be modeled as a series of separate layers, but doing so does not allow the layers themselves to evolve and change thickness and viscosity. This is best done in experiments. On the other hand, however, experiments have the drawback that the surface deformation and geoid anomaly can only be computed by digitizing the temperature fields, which because they are not known in great detail introduce significant uncertainties. But the full visualization of the flow, growth of the crust, and temporal evolution of the whole system far outweigh this disadvantage.

which gives the essential competition between thermal destabilization as measured by the thermal diffusivity (K) and stabilization due to the rate of advancement (V) of the high viscosity front.

By knowing the numerical value of the critical Ra the growth rate can be found for the onset of convection, namely, from (1)

$$V_c = K\left(\frac{\alpha g \Delta T}{\nu K Ra_c}\right)^{1/3} \qquad (2)$$

and from the developing thermal regime, the thickness of the lithosphere at the time of instability can be found.

We have already done this for the paraffins and we wish now to measure Ra_c, V_c and d_c (critical lithosphere thickness) at the onset of convection for the syrup working fluid. Based on the tank thickness, the governing global Rayleigh number is in the range 10^5-10^6, which closely matches that of the earth.

(2.) Paired Fracture Zones: The influence of a single fracture zone on convection was studied numerically by Craig and McKenzie (1986). The role of paired fracture zones is important for understanding the 2000 km geoid anomalies because of the adherence of this anomaly field to the general pattern of major fracture zones (Marsh, et al., 1984).

This can be done experimentally by building a new cooling plate whereby coolant circulation is partitioned into three adjacent parts of the lid. A hot center section bordered by cool regions on

each side, or alternatively the center section can be cooled for some time before commencement of cooling in the adjoining sections. This will establish horizontal as well as vertical temperature gradients to drive the flow. We want to study the spacing of the fracture zones (by moving the partitions within the cooling plate) relative to the dominant spatial scale of flow. To visualize the plan form of this flow we will insert a mirror on the floor of the tank and photograph it through the side of the tank.

(3.) Vertical Viscosity structure: If the flow is confined to a low viscosity channel immediately beneath the lithosphere, the horizontal scale may be greatly limited. Both Robinson and Parson (1988) and Craig and McKenzie (1986) rely on this feature to obtain cell sizes that approximately match the geoid anomalies observed by Haxby and Weissel (1986). The former study further allows continued instability to penetrate the floor of the channel to produce a larger scale flow at late times that will contribute to the background heat flow, elevating the usual plate heat flow at late times.

Such a viscosity structure can be formed in our apparatus by employing two cooling/heating plates (top and bottom) whereby a temperature gradient is maintained across the layer. Establishing a stable linear temperature gradient across the layer (cool at bottom, warm at top) will produce a more viscous floor region. Sudden strong cooling of the roof will initiate convection whose downward penetration will be influenced by the magnitude and thickness of this lower zone. The influence of various viscosity stratifications will

be investigated along with the role of fracture zones in modulating the flow. The relation of fracture zone spacing to the vertical scale of the viscosity field will be investigated in terms of the preferred style of convection.

(4.) 3-D and Temporal Evolution: In numerical experiments the flow is of necessity - in terms of computing expense - almost always approximated by a 2-dimensional representation. In our experiments, however, the flow is clearly unsteady in both two and three dimensions. We would thus like to study the transition from this unsteady flow to a more ordered flow due to the restrictions imposed by the viscosity structure and the fracture zone structure. It may well be that a combination of such features (i.e. fractures and viscosity structure) essentially pin the flow and remove this unsteady nature. In addition, the mainstream flow or absolute motion of the plate size flow may further order the flow as originally suggested by F. Richter and demonstrated experimentally by Richter and Parsons.

In summary, the central theme of this work is to give a dynamic understanding to the origin of a significant part of the geoid field in the Pacific region.

A manuscript is now in preparation for publication covering this year's research.

Bibliography

Booker, J. R. and Stengel, K. C., 1978, Further thoughts on convective heat transport in a variable-viscosity fluid, Jour. Fluid Mechanics, 86, 289-291.

Buck, W. R. and Parmentier, M., 1986, Convection beneath young oceanic lithosphere: implications for thermal structure and gravity, Jour. Geophys, Res., 91, 1961-1974.

Craig, C. H. and McKenzie, D., 1986, The existence of a thin low viscosity layer beneath the lithosphere. Earth Planet. Sci. Letts., 78, 420-426.

Driscoll, M. L. and Parsons, B., 1988, Cooling of the oceanic lithosphere - evidence from geoid anomalies across the Udintsev and Eltanin fracture zones. Earth Planet. Sci. Letts., 288, 289-307.

Fleitout, L. M. and Yuen, D. A., 1984, Secondary Convection and the Growth of the Oceanic Lithosphere, Phys. Earth Planet. Inter., 36, 181-212.

Fleitout, L. M., Froidevaux, C. and Yuen, D., 1986, Active Lithospheric Thinning , Tectonophysics, in press, 1986.

Haxby, W. F., and Weissel, J. K., 1986, Evidence of small scale convection from SEASAT altimeter data, J. Geophys. Res., 91, 3507-3520.

Hinojosa, J. H. and Marsh, B., 1985, Effect of the Lithosphere on the Central Pacific Geoid, EOS Transactions, American Geophysical Union (abstract), 66, 246.

Jaupart, C. and Parsons, B., 1985, Convective Instabilities in a Variable Viscosity Fluid Cooled from Above, Phys. Earth Plant. Inter., 39, 14-32,

Jaupart, C. and Brandeis, G., 1986, The stagnant bottom layer of convecting magma chambers, Earth Planet. Sci. Letts., 80, 183-199.

Marsh, B. and Marsh, J. G., 1976, On Global Gravity Anomalies and Two-scale Mantle Convection, J. Geophys. Res., 81, 5267-5280.

Marsh, B. D., J. G. Marsh, and Williamson, R. G., 1984, On Gravity from SST, Geoid from SEASAT, and Plate Age and Fracture Zones in the Pacific, J. Geophys. Res., 89, 6070-6078.

McAdoo, D. C. and Sandwell, D. T., 1988, On the source of crossgrain lineations in the central Pacific gravity field, EOS, 69, 475.

McKenzie, D. , 1983, The Earth's Mantle, Sci. Am., 246, 67-78.

McKenzie, D., Watts, A., Parson, B. and Roufosse, M., 1980, Planform of Mantle Convection Beneath the Pacific Ocean, Nature, 288, 442-446.

Parsons, B. and McKenzie, D., 1978, Mantle convection and the thermal structure of plates, Jour. Geophys. Res., 83, 4485-4496.

Quareni, F., Yuen, D. A., Sewell, G. and Christensen, U.,1985, High Rayleigh number convection with strongly variable viscosity: A comparison between mean field and two-dimensional solutions, Jour. Geophys. Res., 90, 12633-12644.

Renkin, M. L. and Sandwell, D. T., 1982, Compensation of Swells and Plateaus in the North Pacific: No Direct Evidence for Mantle Convection, EOS, Transaction, AGU (abstract), 67, 362.

Richter, F. M. Natif, H. C. and Daly, S F., 1983, Heat transfer and horizon tally averaged temperature of convection with large viscosity variations, Jour. Fluid Mechanics, 129, 173-192.

Robinson, E. M. and Parsons, B., 1988, Effect of a shallow low-viscosity zone on small scale instabilities under the cooling oceanic plates, Jour. Geophys. Res., 93, 3469-3479.

Sandwell, D. T., and Schubert, G., 1982, Geoid Height-Age Relations from SEASAT Altimeter Profiles Across the Mendocino Fracture Zone, J. Geophys. Res., 87, 3949-3958.

Smith, M. K., 1988, Thermal convection during the directional solidification of a pure liquid with variable viscosity, Jour. Fluid Mechanics, 188, 547-570.

Watts, A., 1976, Gravity and Bathymetry in the Central Pacific Ocean, J. Geophys. Res., 81, 1533.

Watts, A. B., Bodine, J. H. and Ribe, N. M., 1980, Observations of Flexure and the Geological Evolution of the Pacific Ocean Basin, Nature, 283, 532-537.

Yuen, D. A., Pletier, W. R. and Schubert, G., 1981, On the existence of a second scale of convection in the upper mantle, Geophys. Jour. Roy. Astro. Soc., 65, 171-190.

Yuen, D. A. and Fleitout, L., 1984, Stability of the Oceanic Lithosphere with Variable Viscosity: an Initial-value Approach, Phys. Earth Planet. Inter., 34, 173-185.

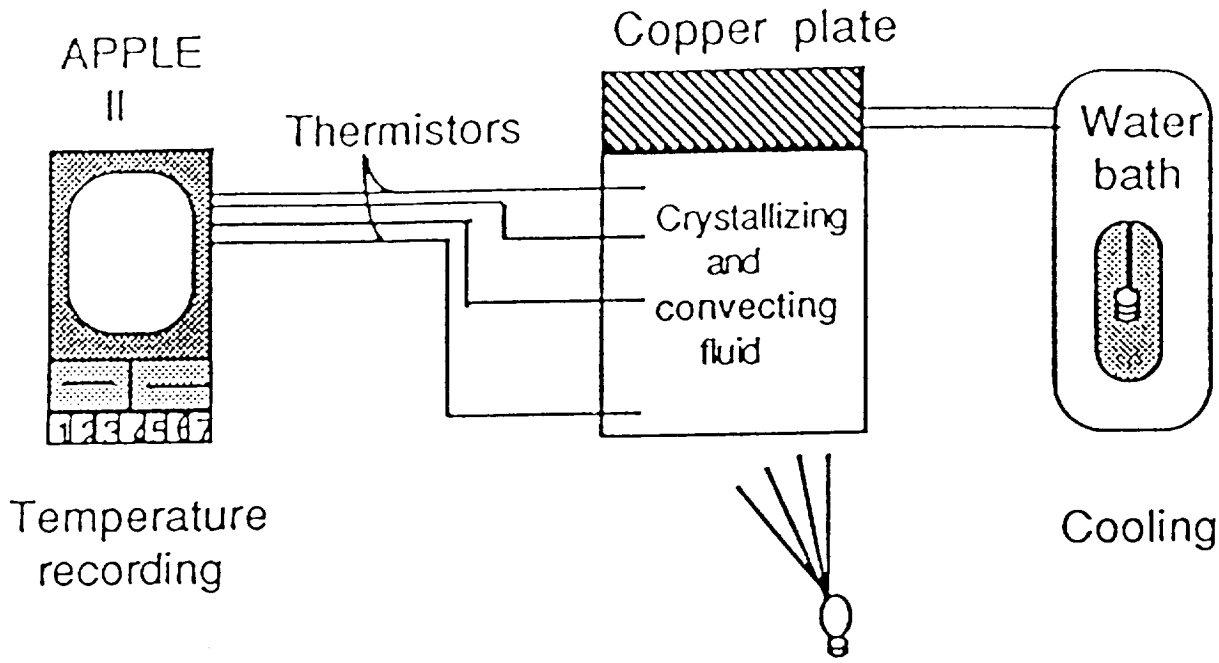

Figure 1: A schematic representation of the experimental setup. A plexiglass tank with a metallic cooling lid holds the viscous fluid. The temperature of the lid is controlled by a water bath. A computer monitors a rack of 8 thermocouples within the fluid. Motion in the fluid is detected by passing a sheet of light through the tank and photographing it at right angles.

Figure 2a: Three stages in cooling molten paraffin from above, showing the progressive growth of an upper rigid crust (white layer) and the onset of plume-like convection (top). At intermediate times, fully developed small scale flow occurs (middle) in only the upper part of the tank. At late stages convection ceases (bottom).

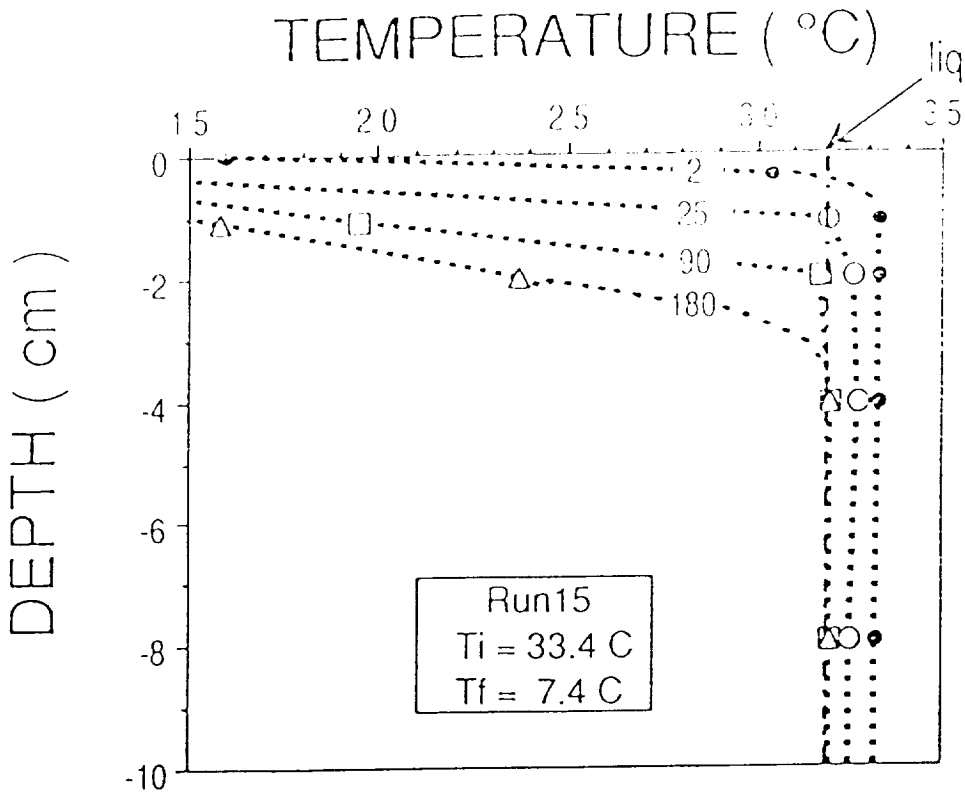

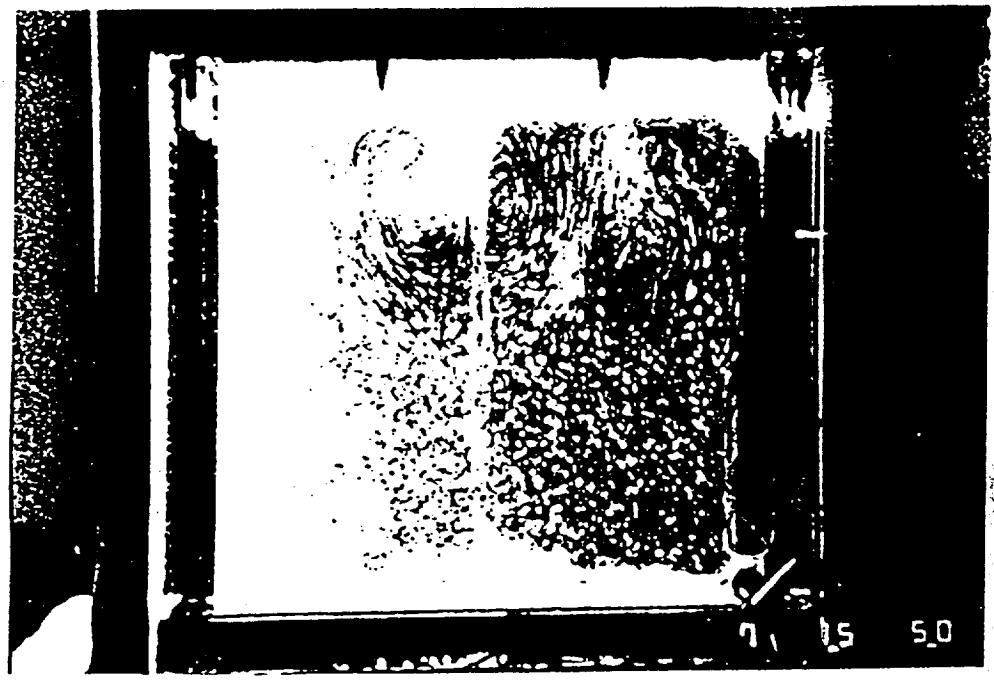

Figure 2b: Evolution of temperature during a typical run. Beginning at above liquidus temperatures, convection ceases when the temperature reaches the liquidus after which cooling is mainly by conduction.

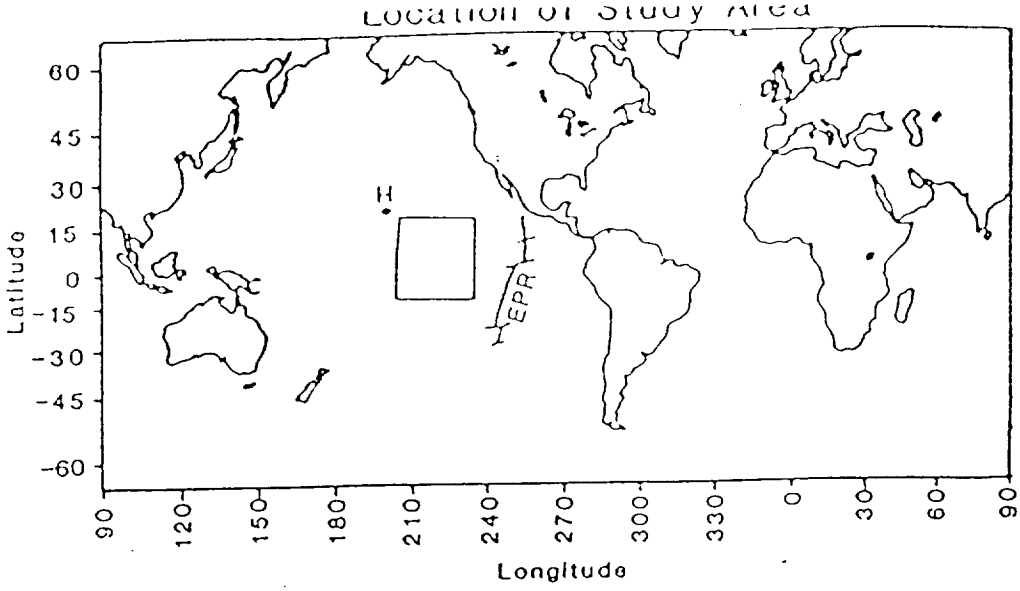

Figure 3. Map showing the location of the study area in the central Pacific Ocean.

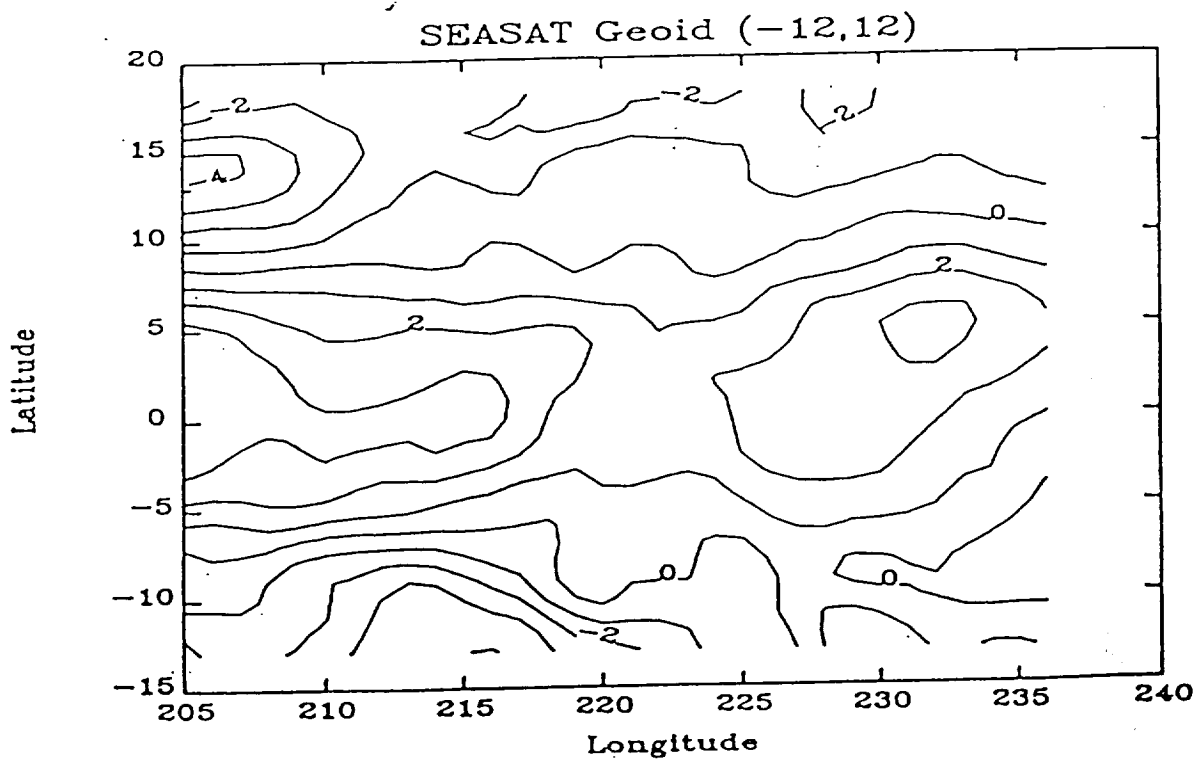

Figure 4a. Contour map showing the high degree and order SEASAT geoid (-12,12) in the study area. Contour interval = 1 m.

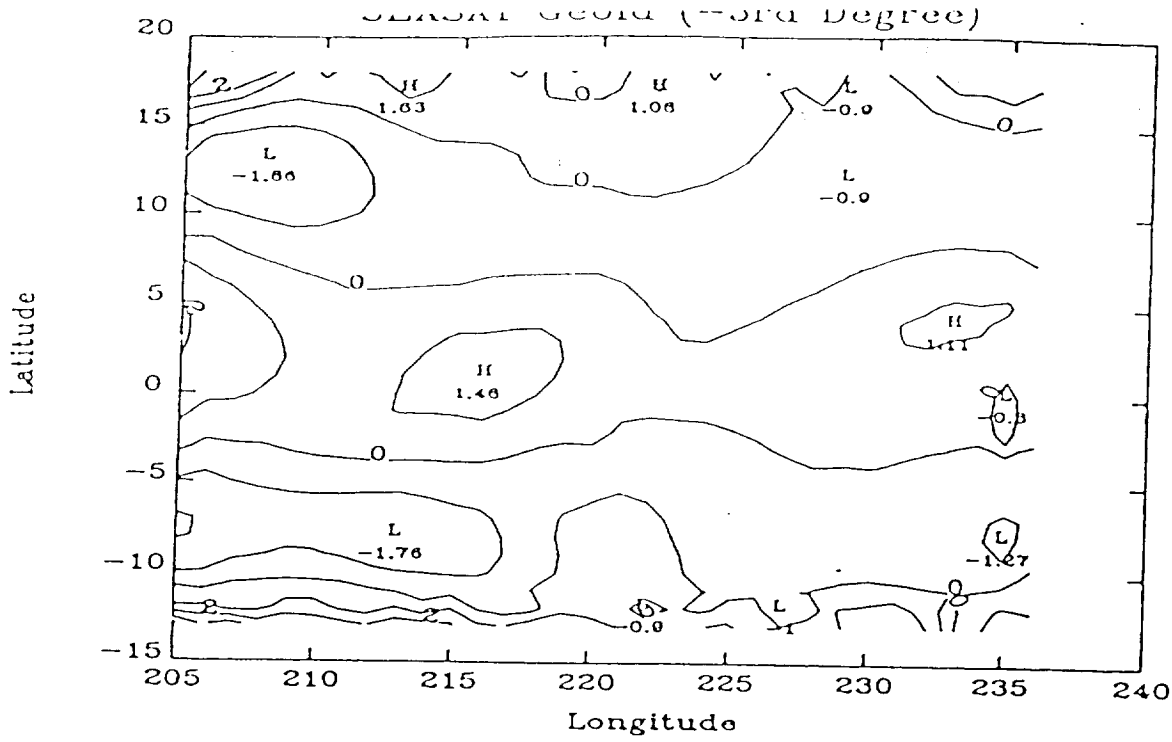

Figure 4b. The resultant geoid field after removing a third degree surface from the full geoid in Figure 2a. Contour interval = 1 m.

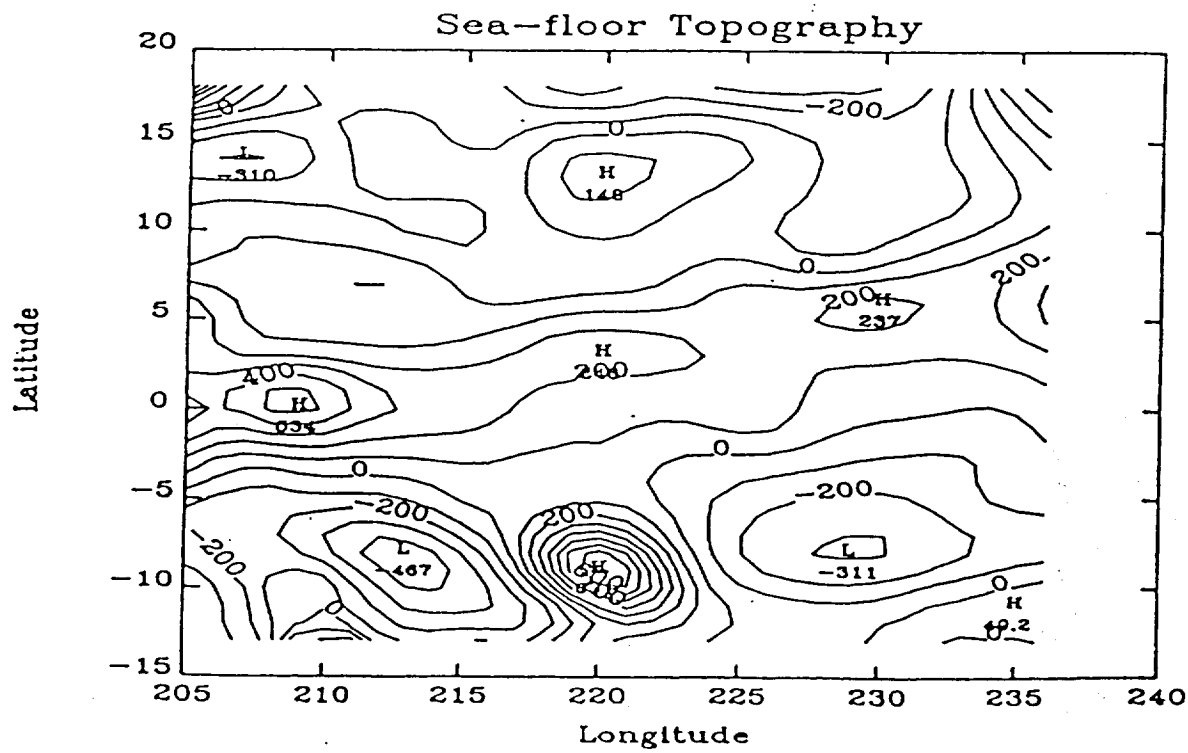

Figure 4c. Contour map showing the sea-floor topography obtained by Gaussian high-pass filtering the bathymetry in the study area. Contour interval = 100 m.

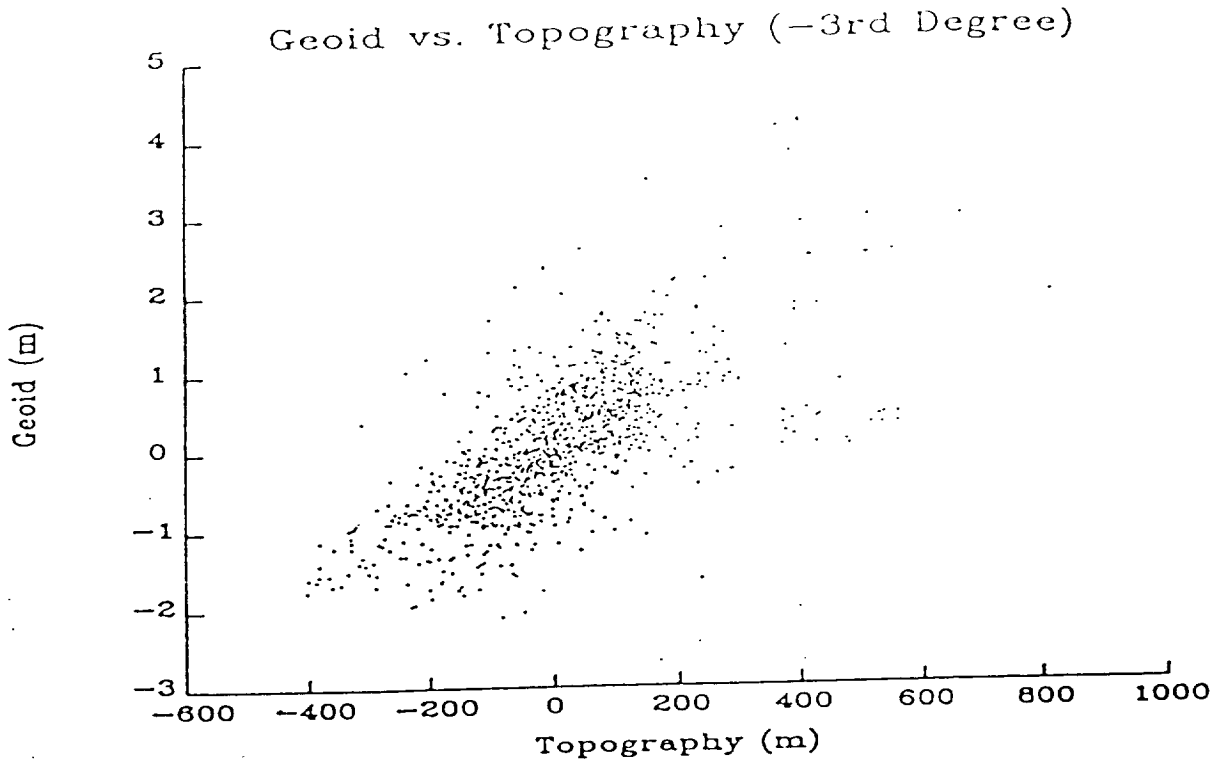

Figure 5. Scatter plot of the geoid (Fig.2b) and topography (Fig.2c).

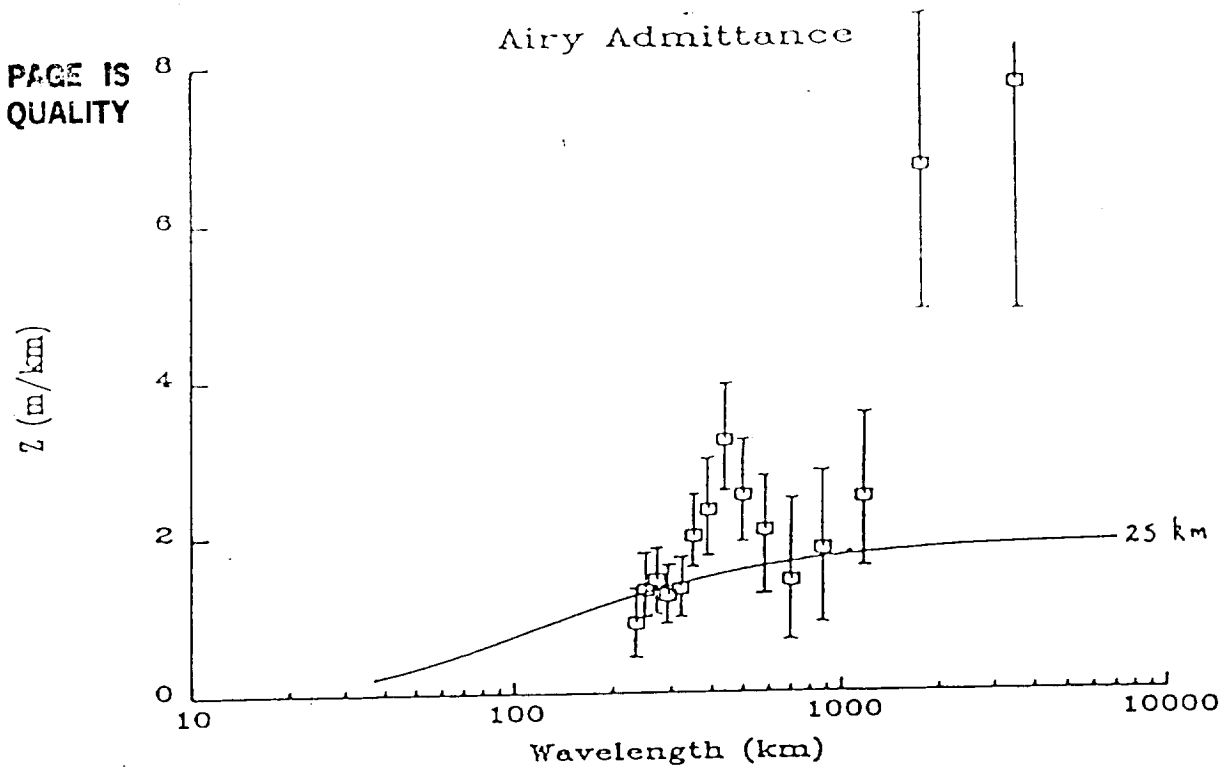

Figure 6a. Comparison of the observed admittance spectrum with the Airy model admittance curve corresponding to a depth of compensation of 25 km.

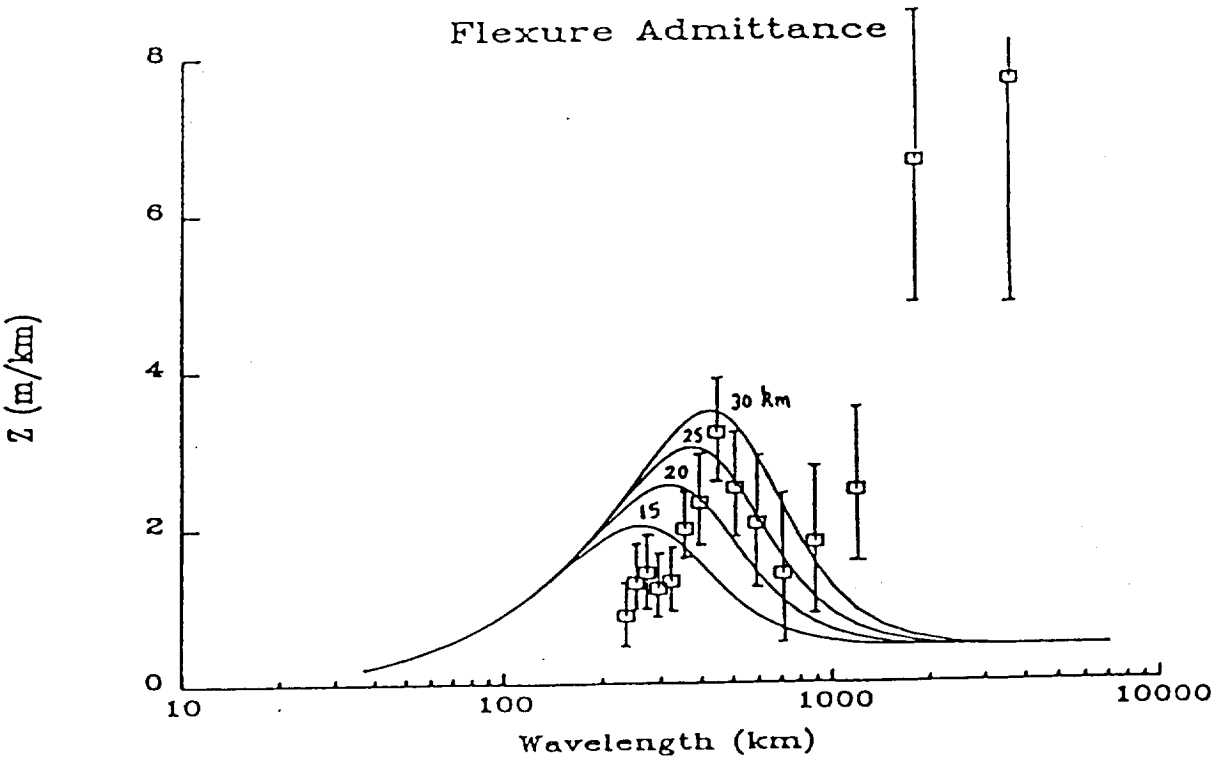

Figure 6b. Comparison of the observed admittance spectrum with flexure model admittance curves for the values of the elastic plate thicknesses shown next to each curve.

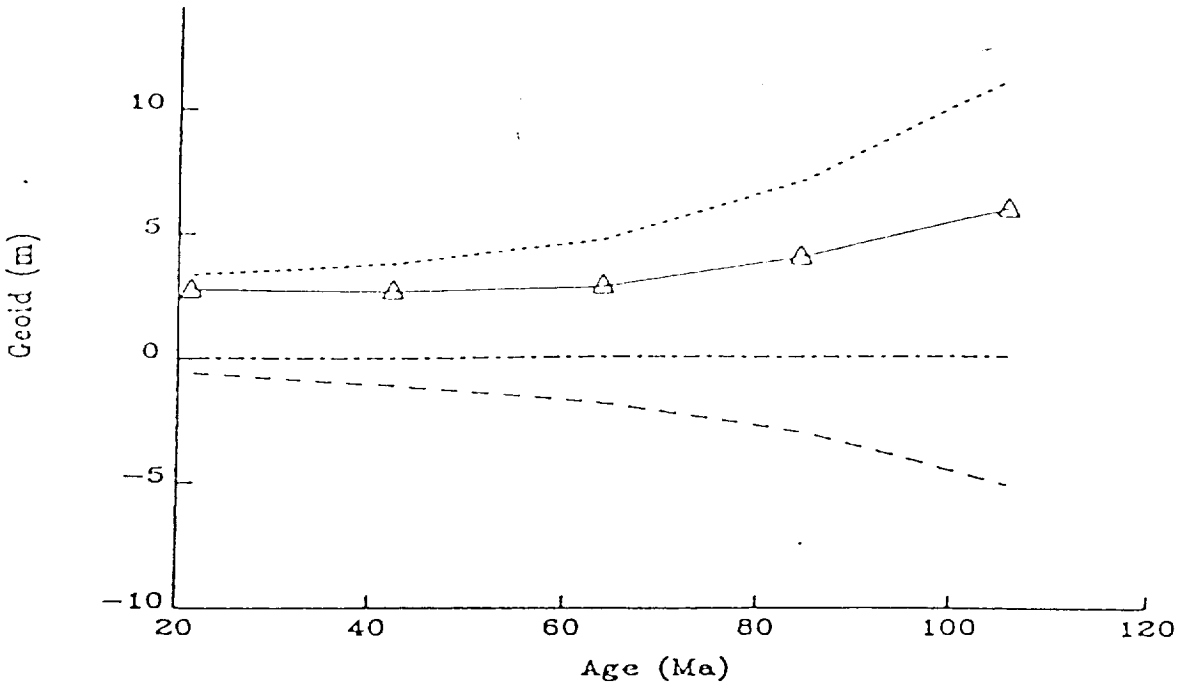

Figure 7a. The geoid components as a function of age for case 1.
The open triangles are the calculated values. The solid line is the total geoid anomaly, the dotted line is the upper-boundary-deformation contribution, the dashed line is the thermal contribution, and the dot-dashed line is the lower-boundary-deformation contribution.

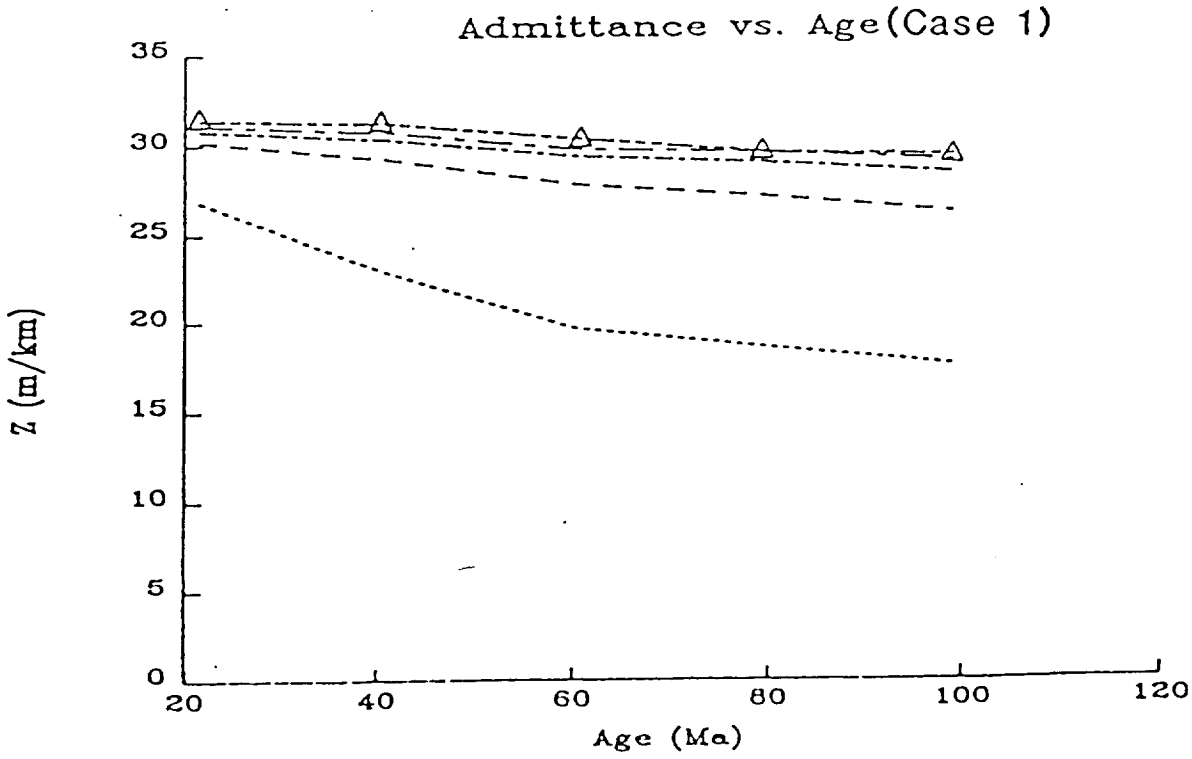

Figure 7b. The admittance as a function of age for case 1 with the different values for the activation energy.

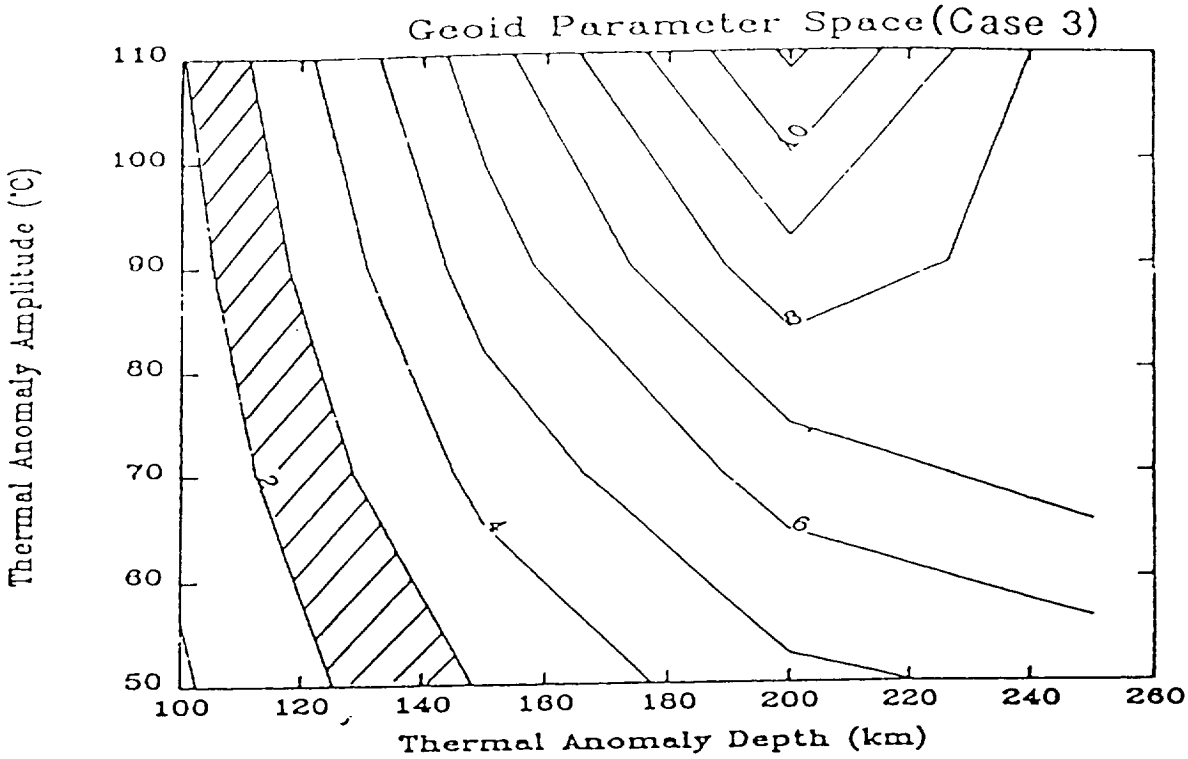

Figure 8 . The parameter space for the predicted geoid anomaly for case 3 in which the fluid layer is cooled from above, the lower boundary temperature is fixed at 1300° C, the Rayleigh number is 585 000, the mean viscosity at T = 1300° C is 1.E22 Poise, the activation energy is 526 kJ/mol, the cut-off temperature is 950° C, and the initial LVZ temperature is 1350° C extending to a depth of 200 km. The thermal perturbation was initially introduced extending from the surface down to a given depth (horizontal axis) and of a given initial amplitude (vertical axis). The values correspond to an age of about 60 Ma. The hatched area corresponds to the range of the observed geoid anomaly. Contour interval = 1 m.